Photosynthesis Research (2005) 84: 339–345 © Springer 2005

Regular paper

Search for intermediates of photosynthetic water oxidation

Juergen Clausen & Wolfgang Junge*
*Biophysik, Universität Osnabrück, 49069 Osnabrück, Germany; *Author for correspondence (e-mail: junge@ uos.de; fax: +49-541-969-2262)*

Received 27 September 2004; accepted in revised form 8 March 2005

Key words: intermediate, photosynthesis, Photosystem II, S-state, water oxidation

Abstract

Photosystem II of cyanobacteria and plants incorporates the catalytic centre of water oxidation. Powered and clocked by quanta of light the centre accumulates four oxidising equivalents before oxygen is released. The first three oxidising equivalents are stored on the Mn_4Ca-cluster, raising its formal oxidation state from S_0 to S_3, and the third on Y_Z, producing $S_3\ Y_Z^{ox}$. From there on water oxidation proceeds in what appears as a single reaction step $(S_3Y_Z^{ox}(H_2O)_2 \rightleftharpoons O_2 + 4H^+ + S_0)$. Intermediate oxidation products of bound water had not been detected, until our recent report on the stabilisation of such an intermediate by high oxygen pressure (NATURE 430, 2004, 480–483). Based on the oxygen titration (half-point 2.3 bar) the standard free-energy profile of a reaction sequence with a single intermediate was calculated. It revealed a rather small difference (-3 kJ mol^{-1}) between the starting state $[S_3Y_Z^{ox}(H_2O)_2$ and the product state $S_0Y_Z + O_2 + 4H^+$. Here we describe the tests for side effects of exposing core particles to high oxygen pressure. We found the reduction of $P_{680}^{+\bullet}$ in ns and the reduction/dismutation of quinones at the acceptor side of PSII both unaffected, and the inhibition of the oxygen evolving reaction by exposure to high O_2-pressure was fully reversible by decompression to atmospheric conditions.

Abbrevations: β-D-M – n-dodecylβ-D-maltoside; Chl – chlorophyll; D1, D2 – core subunits of Photosystem II; ET – electron transfer; DCBQ – 2,5-dichloro-*p-benzoquinone;* FWHM – full width at half maximum; MES – 2-(*N*-morpholino)-ethanesulfonic acid; OEC – oxygen evolving complex; P_{680} – primary electron donor of PS II; PS II – Photosystem II; Q_A, Q_B – bound quinone acceptors in PS II; S_i, $(i = 0 - 4)$ – redox states of the catalytic centre; Y_Z – redox-active tyrosine-161 of D1

Introduction

The oxygen we breathe is produced by Photosystem II (PS II) of cyanobacteria, algae and higher plants. The cofactors of the electron transfer are localised in the two central subunits D1 and D2 of PS II. The oxygen evolving complex (OEC) consists of four Mn-ions, at least one Ca^{2+}, one Cl^-, bound water, amino-acid ligands and a redox-active tyrosine (Y_Z) (Zouni et al. 2001; Ferreira et al. 2004). Powered and clocked by four quanta of light the centre accumulates four oxidising equivalents, giving rise to S_n-states (where *n* indicates the number of stored oxidation equivalents; $n = 0,\ldots,4$) before oxygen is released spontaneously (Joliot et al. 1969; Kok et al. 1970). The first three oxidising equivalents are stored on the Mn_4 Ca-cluster [or on its ligands (Messinger et al. 2001)], raising its formal oxidation state from S_0 to S_3, and the third one on Y_Z, produces $S_3Y_Z^{ox} = S_4$. From there on, water oxidation proceeds in what appears as a single reaction step $(S_3Y_Z^{ox}(H_2O)_2 \rightleftharpoons O_2 + 4H^+ + S_0Y_Z)$. The dark-stable resting state of the OEC is S_1; therefore oxygen evolution of dark adapted samples peaks on the third flash and subsequently on every fourth flash (7th, 11th,…,). Recently, we shifted the equilibrium between the educt ($S_3Y_Z^{ox}(H_2O)_2$), a putative intermediate and the product ($O_2 + 4H^+ + S_0Y_Z$) towards the educt and the intermediate (Clausen and Junge 2004). This aim was reached by increasing the oxygen pressure from 0.21 (i.e. ambient) to 30 bar. Half-suppression occurred at rather low pressure of 2.3 bar, and the maximum was reached between 5 and 10 bar. Hydrostatic pressure alone (19 bar N_2) was without any effect. The calculated small driving force (-3 kJ mol^{-1} under standard conditions) emphasised that PS II operates at the outmost redox span that can be driven by a 680-nm-photon. This conclusion was based on absorption changes at 360 nm. These flash-induced difference signals had to be corrected for oxygen sensitive acceptor-side contributions; i.e. for the decaying signal of the dismutation of the artificial electron acceptor DCBQ (Bögershausen and Junge 1995). In this article, we present evidence that the elevated oxygen pressure had no side-influence on other reactions at the donor- or the acceptor-side of PS II.

Materials and methods

Oxygen evolving PS II core particles were prepared as described in (Clausen et al. 2001b) from modified WT*-cells (Clausen et al. 2001b).

Spectroscopic measurements of electron transfer from the Mn cluster to Y_Z^{ox}

The flash spectroscopic experiments at 360 nm were carried out as described in (Clausen and Junge 2004) (plus supplementary material).

Spectroscopic measurements of electron transfer from Y_Z to $P_{680}^{+\bullet}$

Absorption transients were monitored at a wavelength of 827 nm. Samples (35 μM Chl, 0.08% (w/v) β-DM) contained in the pressure controlled optical cell were repetitively excited with trains of 50 flashes from a Q-switched Nd-YAG laser (wavelength 532 nm, duration 3 ns FWHM, saturating energy, 100 ms between flashes). 1.3 mM 2,5-DCBQ was used as electron acceptor. Four trains of 50 flashes were applied to each sample; 2 min dark adaptation between each cycle. Data were recorded at an analogue bandwidth of 1 GHz, digitised at 4 ns per bin.

Flash induced absorption differences at 402, 425, 465 and 673 nm

Samples (8 μM Chl, 0.06% (w/v) β-DM) contained in the pressure controlled optical cell were excited with a series of three flashes from a Q-switched Nd-YAG laser (wavelength 532 nm, duration 6 ns FWHM, saturating energy, 100 ms between flashes). Each sample was repetitively excited with up to five trains with 2 min dark-adaptation between each train. 200 μM 2,5-DCBQ was used as electron acceptor. Data were recorded at an analogue bandwidth of 100 kHz, digitised at 10 μs per bin.

Results and discussion

The electron transfer involving the MnCa-cluster and Y_Z^{ox} as function of the oxygen pressure

Figure 1a shows the influence of the increased oxygen pressure (20 bar) on the oscillatory pattern of the S-state transitions (Lavergne 1991; Karge et al. 1997; Haumann et al. 1997a) at 360 nm. The signals of the first two flashes (S-state transitions $S_1 \Rightarrow S_2$ and $S_2 \Rightarrow S_3$) were virtually unaffected. The small difference in the positive jump upon the first flash was attributable to a different percentage of centres that were incompetent in oxygen evolution (Lavergne 1991; Hundelt et al. 1998). The striking differences were obvious upon the third and the fifth flash. The control sample (black trace) exhibited a large negative signal upon the third flash, it reverted the positive absorption changes during flash nos. 1 and 2. This large negative signal represents the reduction of the OEC under evolution of oxygen. The transition from S_0 to S_1 does not show a difference signal at this wavelength (Lavergne 1991), in Figure 1a this was evident from the transient upon the fourth flash in the series. The positive absorption difference upon the fifth flash (black trace) represents the oxidation from $S_1 \Rightarrow S_2$ at the beginning of the second cycle. Under 20 bar oxygen (grey transient) the reduction of the OEC upon the third flash was suppressed and the extent of large negative signal

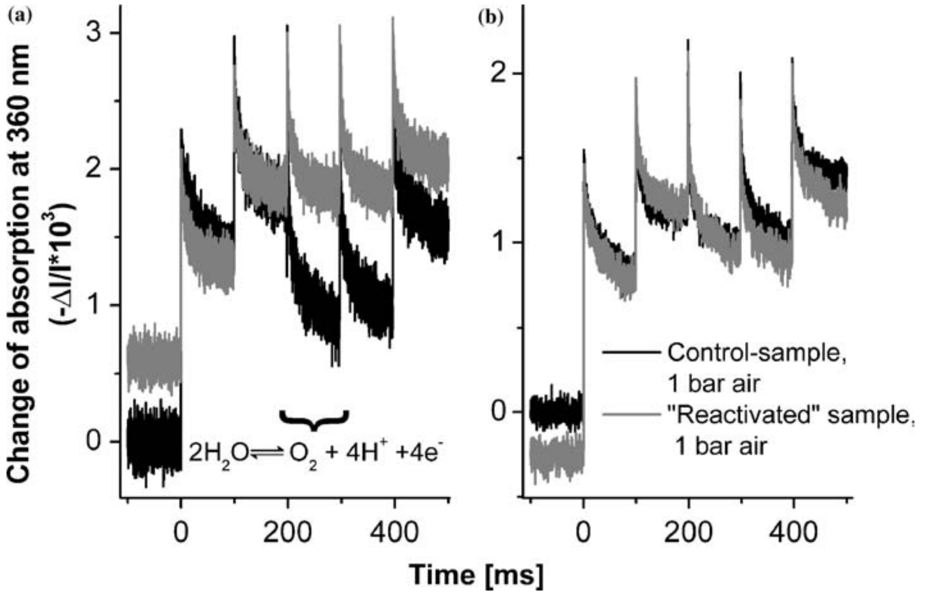

Figure 1. (a) UV-absorption transients at a wavelength of 360 nm of dark adapted Photosystem II core particles under excitation with five short laser flashes. Black trace: air, grey trace: 20 bar oxygen. The 'undershoot' after the third flash (black trace) reflects the relaxation of the four-fold oxidised catalytic centre culminating in the release of oxygen. The extents of the positive amplitude upon the third flash were normalised. Three transients averaged (reproduced from Clausen and Junge 2004). (b) Reversibility of the inhibition by 20 bar oxygen. PSII core complexes were incubated for 20 min under 20 bar oxygen and decompressed for 145 min. The normal (black transient) oscillatory behaviour under excitation of dark adapted material with a group of light flashes was restored (grey transient). The extents of the positive amplitude upon the third flash were normalised. Five semi-repetitive measurements (2 min dark adaptation between each train). Time resolution 100 µs/point.

was decreased. This decrease was ascribed to the stabilisation of the intermediate (for details see Clausen and Junge 2004). The pattern of absorption transients in the presence of 20 bar oxygen proved that the oscillations of the S-states were inhibited to a large extent from the third flash on. The large positive absorption change on the fifth flash (due to the $S_1 \Rightarrow S_2$ transition under normal conditions, see above) was absent.

On the reversibility of the effects of high oxygen pressure

The inhibition of core-complexes by 20 bar oxygen was reversible. After exposition of PS II core complexes to 20 bar oxygen, as described in the Materials and methods section (without addition of DCBQ), the sample was decompressed and reequilibrated for 2.5 h with the standard atmosphere (21/2 h stirring on ice under 1 bar air). The oscillatory pattern of the samples was restored (Figure 1b). The large negative amplitude upon the third flash was identical in the control sample (black) and in the reactivated sample (grey transient). Moreover, the positive absorption change upon the fifth flash ($S_1 \Rightarrow S_2$ of the second cycle, see above) was restored in the reactivated sample, indicating the progression of the sample beyond the S_3-state. Again, the positive jump in the first flash varied between the samples (see above). The oxygen evolution under continuous illumination of the reactivated sample was 70–80% compared to the control sample.

We checked if the equilibration of oxygen between the gas phase and buffer was complete under the chosen conditions. Therefore we measured the decline of the negative amplitude at 20 bar oxygen pressure under various incubation conditions. The extent of the decline of the negative amplitude was identical, if the core complexes were incubated for 10, 20 or 30 min. As a consequence, the core-complexes were incubated for 20 min under 20 bar in all subsequent experiments. We checked, whether the decline of the negative amplitude was the same, if the buffer (before sample-injection) was equilibrated for 10 min or for up to 60 min. Again both results were identical. These results proved that the buffer was fully equilibrated. Moreover, this proved that the inhibition of the core complexes was completed under the chosen conditions and that the decline of the negative amplitude was not caused by a time-dependent degradation of the sample under elevated oxygen pressure.

Titration of the transition $S_4 \Rightarrow S_0$ by elevated oxygen pressure

We titrated the large negative UV-amplitude as a function of the pressure and the gas composition (Clausen and Junge 2004). The data were analysed under the assumption of a consecutive reaction scheme: $\mathrm{A} \underset{b}{\overset{a}{\rightleftharpoons}} \mathrm{B} \underset{d}{\overset{c}{\rightleftharpoons}} \mathrm{C} + \mathrm{O}_2 +$ protons. The initial concentration of A_0 was 1 and the initial concentration of B_0 and C_0 was 0. In the equilibrium K_{AB} was $\frac{B_\infty}{C_\infty} = \frac{a}{b}$ and K_{BC} was $\frac{C_\infty}{B_\infty} = \frac{c}{dp}$. The absorption change in dependence of the oxygen-pressure was fitted under the assumption of a half-absorbing intermediate (HAI) or, alternatively, a nonabsorbing intermediate (NAI). The new equilibrium was $A_\infty = \frac{1}{1+\frac{a}{b}+\frac{c}{d*p}*\frac{a}{b}}$ for NAI and $A_\infty + 1/2B_\infty = \frac{1+\frac{1}{2}*\frac{a}{b}}{1+\frac{a}{b}*\left(1+\frac{c}{d*p}\right)}$ for HAI. The ratio of rate constants was determined from the lines of best fit (not shown here, but see Clausen et al. 2004) and the ΔG-values were calculated, according to$\Delta G = -RT \ln K$. The results are summarised in Table 1. The calculated Gibbs-energy drop was rather small, confirming that PS II operates at the outmost redox span that can be driven by a 680-nm-photon.

From the ratio of rate constants and the measured effective half-decay time of the spectroscopic transient of the $S_3 \Rightarrow S_0$ transition (0.8 ms at 20 bar oxygen) the absolute values of the rate constants were calculated (under assumption that the reaction from the intermediate to the product is fully inhibited). They were $a = 144\ \mathrm{s}^{-1}$, $b = 722\ \mathrm{s}^{-1}$ for NAI and $a = 289\ \mathrm{s}^{-1}$, $b = 578\ \mathrm{s}^{-1}$ for HAI. Please note that these values had been mixed up *vice versa* in our recent publication (Clausen and Junge 2004).

The decay of the educt $S_3Y_Z^{ox}(H_2O)_2$ to the product S_0Y_Z was simulated according to the following reaction scheme: $A \underset{b}{\overset{a}{\rightleftharpoons}} B \underset{d}{\overset{c}{\rightleftharpoons}} C$. With the determined absolute rate constants a and b and the determined ratio of c/d, the decay at 0.21 bar was simulated (under assumption of a 100-fold faster rate constant c) and compared with the observed half-decay time [≈1.3 ms (Haumann et al. 1997b; Hundelt et al. 1998; Clausen et al. 2001a, 2004)]. The best consensus was achieved under the assumption of a half-absorbing intermediate (HAI; $\tau_{1/2} = 2.3$ ms; Figure 2), corroborating our recent assignment of the stabilised intermediate to $S_2 \bullet H_2O_2$ (Clausen and Junge 2004). The simulated half decay-time under the assumption of a NAI was 4.67 ms. The small difference between the simulated results with a HAI ($\tau_{1/2} = 2.3$ ms) and the measured results ($\tau_{1/2} \approx 1.3$ ms) was probably attributable to the imprecise determination of the effective rate constant at 20 bar oxygen (low signal-to-noise-ratio; data not shown). Moreover, the absolute rate constants were determined under the assumption (Clausen and Junge 2004) that the equilibrium concentration of C was zero at 20 bar oxygen. In fact, the simulations showed that about 10% of C was still formed under 20 bar oxygen. Taking this into account, the effective half-decay time is shorter than 0.8 ms (see above), if no C is formed anymore, resulting in higher values for the absolute rate constants a and b. The increase of a and b by a factor of only 1.7 would already decrease the half-decay time for A to $\tau_{1/2} = 1.2$ ms at 1 bar

Table 1. Results of the redox titration of the oxygen-evolving step

	Half-suppression	Ratio of rate constants a/b	Ratio of rate constants c/d	$\Delta G'$ (1 bar O_2)	ΔG (0.21 bar O_2)
NAI	2.31 bar	0.2	13.6 bar	$\Delta G'_{\mathrm{A}\to\mathrm{B}} = 3.9\,\mathrm{kJ\,mol^{-1}}$ $\Delta G'_{\mathrm{B}\to\mathrm{C}} = 6.3\,\mathrm{kJ\,mol^{-1}}$	$\Delta G_{\mathrm{A}\to\mathrm{B}} = 3.9\,\mathrm{kJ\,mol^{-1}}$ $\Delta G_{\mathrm{B}\to\mathrm{C}} = 10.2\,\mathrm{kJ\,mol^{-1}}$
HAI	2.3 bar	0.5	6.8 bar	$\Delta G'_{\mathrm{A}\to\mathrm{B}} = 1.7\,\mathrm{kJ\,mol^{-1}}$ $\Delta G'_{\mathrm{B}\to\mathrm{C}} = 4.7\,\mathrm{kJ\,mol^{-1}}$	$\Delta G_{\mathrm{A}\to\mathrm{B}} = 3.9\,\mathrm{kJ\,mol^{-1}}$ $\Delta G_{\mathrm{B}\to\mathrm{C}} = 8.5\,\mathrm{kJ\,mol^{-1}}$

A = educt $S_3Y_Z^{ox}(H_2O)_2$; B = intermediate; C = products $S_0Y_Z + O_2$ + protons.

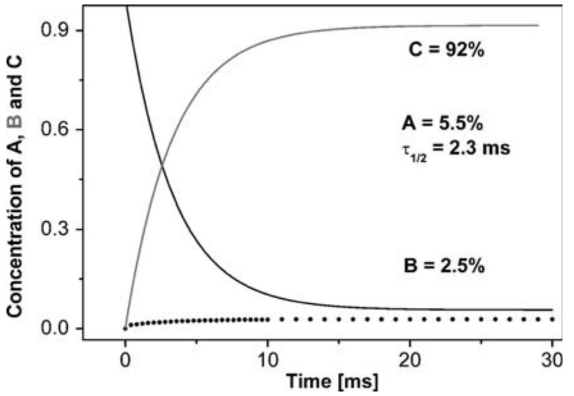

Figure 2. Simulation of the decay of A in time under assumption of a HAI (black line). The half-decay time for a was 2.3 ms. $a/b = 0.5$, $c/d = 6.8$ bar. $a = 289\ \mathrm{s}^{-1}$, $b = 578\ \mathrm{s}^{-1}$, $c = 28890\ \mathrm{s}^{-1}$. The back reaction $C \rightleftharpoons B$ was simulated with the pseudo-first order rate constant $d'[d' = d * p(O_2)]$. The time dependent course of the concentrations of the intermediate B (dotted) and the product C (grey line) were also displayed.

air in agreement with the spectroscopic data (for HAI). On the contrary, a 1.7-fold increase of the determined absolute rate constants for NAI would result in a half-decay time of 2.84, which is still not in line with the experimental data.

The presence of a peroxo-intermediate in the final reaction has been postulated since 1978 (Renger 1978). However, the identity of the stabilised intermediate still remains to be characterised. Further experiments to clarify this point are in preparation.

Reduction of $P_{680}{}^{+\bullet}$

The reduction of $P_{680}^{+\bullet}$ was measured at 827 nm under repetitive excitation of the sample. The transients are shown in Figure 3. The decay of transients in control samples (Figure 3a) was fitted (solid line) with two exponentially decaying phases with half-decay times of 23 ns (47%), 272 ns (16%), and an offset of a µs-phase (36%, $\tau_{1/2} > 2\mu$s). Similar half times have been reported previously for chloroplasts and PS II preparations from spinach (Brettel and Witt 1983), PS II core-complexes from *Synechocystis* sp. PCC 6803 (Hundelt et al. 1998; Clausen et al. 2001b) and for PS II core particles from *Thermosynechococcus elongatus* (Schlodder et al. 1985). Data fit obtained with PS II core particles under 20 bar oxygen (Figure 3b) revealed unaffected half-decay times: 25 ns (52%), 250 ns (14%), >2 µs (34%). Only the overall amplitude decreased to 73% in comparison to the control sample. The unaffected half-decay times of $P_{680}^{+\bullet}$-reduction and the unchanged fraction of the respective phases implied that Y_Z^{ox} was reduced in the 100 ms dark-time between the flashes by alternative, intrinsic electron donors of PS II. Even the proton relax-

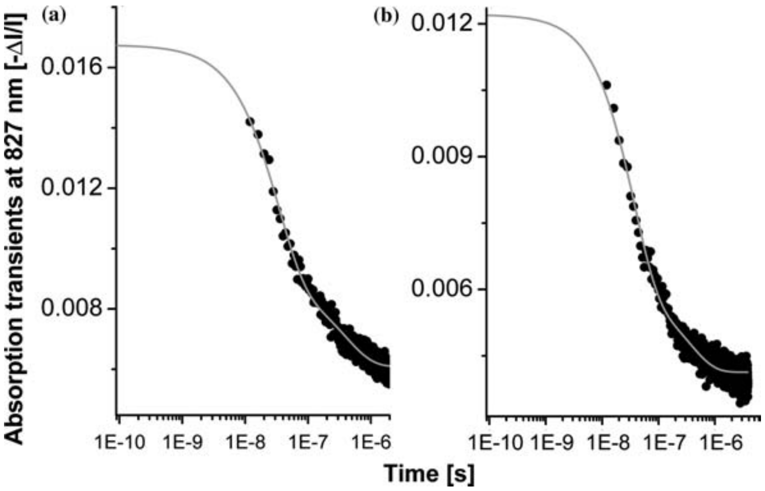

Figure 3. The reduction of $P_{680}^{+\bullet}$ was unaffected between control-samples and samples under 20 bar oxygen pressure. 600 transients averaged. (a) bar air [0.21 bar p(O_2)]. The data (closed circles) were fitted (solid lines) with half-time of 23 ns (47%), 272 ns (16%) and >2 µs (36%). (b) 20 bar oxygen pressure. The fit results were 25 ns (52%), 250 ns (14%) and >2 µs (34%).

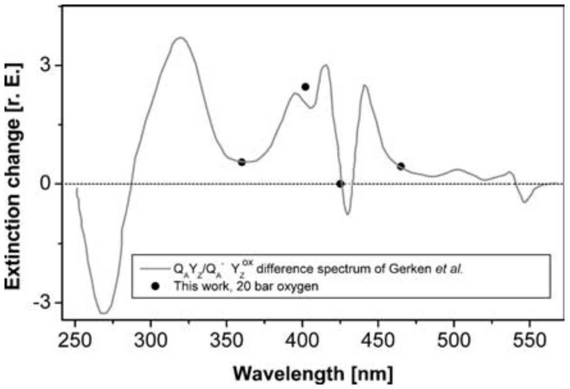

Figure 4. Comparison of the difference spectrum of $Q_AY_Z/Q_A^{-\bullet}Y_Z^{ox}$ (Gerken et al. 1989) with the difference amplitudes of the fast jump under 20 bar oxygen pressure (see text).

ation, which is attributed to the μs-phases (Krishtalik 1995; Cherepanov et al. 1998), was unaffected. The unaffected reduction of $P_{680}^{+\bullet}$ explains the unchanged acceptor-side reaction as visible in Figure 1. The positive jump upon each flash in Figure 1 represented the fast reduction of Q_A by P_{680} ($\tau_{1/2} \approx 200$ ps; Rutherford 1989; Diner and Babcock 1996) via phaeophytin and the following reduction of the artificial electron acceptor DCBQ (Bögershausen and Junge 1995). The positive jump was still visible upon the flashes four and five, when the progression of the OEC was inhibited at 20 bar oxygen pressure.

Influence of elevated oxygen pressure on the flash-induced absorption differences at other wavelengths

Our preliminary results on the influence of the elevated oxygen pressure at other wavelengths are reported here. We measured the flash-induced absorption difference at 402, 425, 465 and 673 nm. For the preliminary measurements repetitively dark-adapted samples were used. After each train of three flashes, the samples were dark adapted for 2 min. This flash-regime delivered good results under control conditions (WT*, 1 bar air) (Clausen et al. 2001a, b; 2004) with only minor damping of the oscillations. The flash induced absorption differences were identical between control samples and samples under 20 bar oxygen at 402, 465 and 673 nm on all three flashes. This proved that PS II was generally intact despite the exposition to 20 bar oxygen. A striking difference was visible on all three flashes at 425 nm, even in long-time dark adapted samples: aside from the fast reduction of Q_A an additional slow phase ($\tau_{1/2} = 100$ μs) was visible under 20 bar oxygen (data not shown). This has to be examined in detail in future experiments. The signal-to-noise-ratio was not optimised in this preliminary measurements. Nevertheless, the amplitude of the fast positive jump, caused by the fast reduction of Q_A (see above) and the oxidation of Y_Z, was analysed. These preliminary results were in satisfactory agreement with the difference spectrum reported by (Gerken et al. 1989). The spectra were normalised to the flash-induced absorption difference at 360 nm (Figure 4). The data of Gerken et al. did not range to 673 nm. We measured a strong negative absorption-difference at 673 nm in agreement with other $Q_AY_Z/Q_A^{-\bullet}Y_Z^{ox}$ difference spectra (van Gorkom 1974; Schatz and van Gorkom 1985; Hillmann and Schlodder 1995; Haumann et al. 1996).

Conclusions

Besides the reversible inhibition by high oxygen pressure of the terminal oxygen evolving transition of the water oxidase $S_3Y_Z^{ox}(H_2O)_2 \Rightarrow B \Rightarrow S_0Y_Z + O_2 +$ protons, we did not observe any side effects on other electron transfers in PS II, namely the reduction of $P_{680}^{+\bullet}$ and the reduction of Q_A and the subsequent reactions with the added quinone acceptor (DCBQ). This corroborated the conclusion drawn in the preceding article (Clausen and Junge 2004) that high-oxygen pressure stabilised a (peroxo?) intermediate. This novel approach has paved the way to characterise the chemical nature of intermediates of photosynthetic water oxidation.

Acknowledgements

The authors are grateful to Hella Kenneweg for excellent technical assistance, Holger Heine for advise on the construction of the pressure cell, Prof. Rick Debus for the cooperation on *Synechocystis*, and Drs Ralf Ahlbrink and Armen Mulkidjanian for fruitful discussions and help. This work was financially supported by the Deutsche Forschungsgemeinschaft (Ju97/15-1), the Fonds der Chemischen Industrie and the Land Niedersachsen.

References

Bögershausen O and Junge W (1995) Rapid proton transfer under flashing light at both functional sides of dark adapted Photosystem II core particles. Biochim Biophys Acta 1230: 177–185

Brettel K and Witt HT (1983) Reduction kinetics of the photooxidized chlorophyll a_{II} in chloroplasts measured in the nanosecond range at 837 nm under repetitive flash excitation. Photobiochem Photobiophys 6: 253–260

Cherepanov DA, Drevenstedt W, Krishtalik LI, Mulkidjanian A and Junge W (1998). Protein relaxation and kinetics of $P_{680}{}^{+}$ reduction in Photosystem II. In: Garab G (ed) Photosynthesis: Mechanisms and Effects, pp 1073–1076 Kluwer Academic Publishers, Dordrecht, The Netherlands

Clausen J and Junge W (2004) Detection of an intermediate of photosynthetic water oxidation. Nature 430: 480–483

Clausen J, Winkler S, Hays AMA, Hundelt M, Debus RJ and Junge W (2001a) Mutations D1-E189K, R and Q of *Synechocystis* sp. PCC6803 are without influence on ns-to-ms electron transfer between OEC-Y_z-P_{680} in Photosystem II. In: PS2001 Proceedings – 12th International Congress on Photosynthesis, pp 1–5. Csiro Publishing, Collingwood, Australia

Clausen J, Winkler S, Hays AMA, Hundelt M, Debus RJ and Junge W (2001b) Photosynthetic water oxidation: mutations of D1-Glu189K, R and Q of *Synechocystis* sp. PCC6803 are without any influence on electron transfer rates at the donor side of Photosystem II. Biochim Biophys Acta 1506: 224–235

Clausen J, Debus RJ and Junge W (2004) Time-resolved oxygen production by PS II: chasing chemical intermediates. Biochim Biophys Acta 1655: 184–194

Diner BA and Babcock GT (1996). Structure, dynamics, and energy conversion efficiency in photosystem II. In: Ort DR and Yocum CF (eds) Oxygenic Photosynthesis: the Light Reactions, pp 213–247. Kluwer Academic Publishers, Dordrecht, The Netherlands

Ferreira KN, Iverson TM, Maghlaoui K, Barber J and Iwata S (2004) Architecture of the photosynthetic oxygen-evolving center. Science 303: 1831–1838

Gerken S, Dekker JP, Schlodder E and Witt HT (1989) Studies on the multiphasic charge recombination between chlorophyllA_{II}^{+} (P-680^{+}) and plastoquinone Q_A^{-} in Photosystem II complexes. Ultraviolet difference spectrum of Chl-a_{II}^{+}/Chl-a_{II}. Biochim Biophys Acta 977: 52–61

Haumann M, Drevenstedt W, Hundelt M and Junge W (1996) Photosystem II of green plants: oxidation and deprotonation of the same component (histidine?) on S_1^*—> S_2^* in chloride depleted centers as on S_2— > S_3 in controls. Biochim Biophys Acta 1273: 237–250

Haumann M, Bögershausen O, Cherepanov DA, Ahlbrink R and Junge W (1997a) Photosynthetic oxygen evolution: H/D isotope effects and the coupling between electron and proton transfer during the redox reactions at the oxidizing side of Photosystem II. Photosynth Res 51: 193–208

Haumann M, Hundelt M, Jahns P, Chroni S, Bögershausen O, Ghanotakis D and Junge W (1997b) Proton release from water oxidation by Photosystem II: similar stoichiometries are stabilized in thylakoids and core particles by glycerol. FEBS Lett. 410: 243–248

Hillmann B and Schlodder E (1995) Electron transfer reactions in Photosystem II core complexes from *Synechococcus* at low temperature - difference spectrum of $P_{680}^{+}Q_A^{-}/P_{680}Q_A$ at 77 K. Biochim Biophys Acta 1231: 76–88

Hundelt M, Hays AM, Debus RJ and Junge W (1998) Oxygenic Photosystem II: the mutation D1-D61N in *Synechocystis* sp PCC 6803 retards S-state transitions without affecting electron transfer from Y_Z to PÜ$_{680}^{+}$. Biochemistry 37: 14450–14456

Joliot P, Barbieri G and Chabaud R (1969) A new model of photochemical centers in system-2. Photochem Photobiol 10: 309–329

Karge M, Irrgang KD and Renger G (1997) Analysis of the reaction coordinate of photosynthetic water oxidation by kinetic measurements of 355 nm absorption changes at different temperatures in Photosystem II preparations suspended in either H_2O or D_2O. Biochemistry 36: 8904–8913

Kok B, Forbush B and McGloin M (1970) Cooperation of charges in photosynthetic O_2 evolution – I. A linear four-step mechanism. Photochem Photobiol 11: 457–475

Krishtalik LI (1995) Fast electron transfers in photosynthetic reaction centre: effect of the time-evolution of dielectric response. Biochim Biophys Acta 1228: 58–66

Lavergne J (1991) Improved UV–visible spectra of the S-transitions in the photosynthetic oxygen-evolving system. Biochim Biophys Acta 1060: 175–188

Messinger J, Robblee JH, Bergmann U, Fernandez C, Glatzel P, Visser H, Cinco RM, McFarlane KL, Bellacchio E, Pizarro SA, Cramer SP, Sauer K, Klein MP and Yachandra VK (2001) Absence of Mn-centered oxidation in the S-2 → S-3 transition: implications for the mechanism of photosynthetic water oxidation. J Am Chem Soc 123: 7804–7820

Renger G (1978). Theoretical studies about the functional and structural organization of the photosynthetic oxygen evolution. In: Metzner H (ed) Photosynthetic Oxygen Evolution, pp 229–248. Academic Press, London

Rutherford AW (1989) Photosystem II, the water-splitting enzyme. Trends Biochem Sci 14: 227–232

Schatz GH and Gorkom HJvan (1985) Absorbance difference spectra upon charge transfer to secondary donors and acceptors in Photosystem II. Biochim Biophys Acta 810: 283–294

Schlodder E, Brettel K and Witt HT (1985) Relation between microsecond reduction kinetics of photooxidized chlorophyll a_{II} (P-680) and photosynthetic water oxidation. Biochim Biophys Acta 808: 123–131

Van Gorkom HJ (1974) Identification of the reduced primary electron acceptor of Photosystem II as a bound semiquinone anion. Biochim Biophys Acta 347: 439–442

Zouni A, Witt HT, Kern J, Fromme P, Krauss N, Saenger W and Orth P (2001) Crystal structure of Photosystem II from *Synechococcus* elongatus at 3.8 Å resolution. Nature 409: 739–743